

Quantum chemical study of the structure and energetics of $\text{Li}^+ \cdot 4\text{H}_2\text{O}$ and $\text{Li}^+ \cdot 6\text{H}_2\text{O}$ clusters and the influence of electric field

Christopher D. Daub,^{*,†} Per-Olof Åstrand,[†] and Fernando Bresme^{‡,†}

Department of Chemistry, Norwegian University of Science and Technology (NTNU), Trondheim, Norway NO-7491, and Department of Chemistry, Imperial College London, SW7 2AZ, London, UK

E-mail: christopher.daub@ntnu.no

Abstract

The optimized geometries and binding energies of small clusters of lithium ions and water have been computed using density functional theory. We have carefully tested for effects such as basis set superposition error and basis set extrapolation. We considered the contribution of zero-point vibrational energy, and for small systems we compared to coupled-cluster calculations. Our findings give support for the stability of a cluster with four water molecules in an S_4 symmetric arrangement around the Li^+ ion, rather than a 6-coordinated structure as seen in aqueous clusters with sodium or calcium ions. We also investigate the effect of an applied electric field on the structure of these clusters. We find that an electric field strength of $\sim 0.5 \text{ V/\AA}$ is sufficient to break the symmetry of the S_4 structure and stabilize a cluster configuration with three water

*To whom correspondence should be addressed

[†]NTNU

[‡]Imperial College

molecules bound to the ion and an additional molecule in the second solvation shell. This cluster remains the global minimum configuration at field strengths $\gtrsim 0.15$ V/Å. A similar procedure starting from 6-coordinated $\text{Li}^+ \cdot 6\text{H}_2\text{O}$ shows a transition to 5- and 4-coordinated clusters at field strengths ~ 0.2 V/Å and ~ 0.3 V/Å respectively, with the 4-coordinated structure being the global minimum even in the absence of the field. Our findings are relevant to understanding the behaviour of the Li^+ ion in aqueous environments at equilibrium, under strong electric fields, and/or in interfacial regions where field gradients are significant.

1 Introduction

It has long been established that the surface tensions of aqueous solutions rise with increasing concentration,¹ after going through a minimum at millimolar concentrations.² At a molecular level this can be explained if the ions have a greater tendency to lie in the bulk solution rather than at the interface; if the bulk solution has higher cohesive energy due to the presence of ions but the surface energy remains unchanged, then surface tension will increase. The simple theory of Onsager and Samaras used arguments from continuum electrostatics to show that point charges should avoid interfaces between two media with different dielectric constants.³ Although this theory could not explain the ion-specific differences in surface tensions, for example their greater sensitivity to different anions than cations, little advancement was made for many years.

More recently a combination of simulation⁴⁻⁹ and experimental¹⁰⁻¹² results have made great progress in explaining some of the ion-specific trends in the surface tension data. These advances were largely driven by the realization that surprising amounts of bromide chemistry were occurring in sea salt aerosols, despite the relatively low concentration of bromide in sea water.¹³ These results demonstrated that the simple picture where all ions avoid the interfacial region is incomplete. Instead, the current consensus is that among the simple monoatomic halogens, larger anions like Br^- and I^- have a tendency to populate

the interface, although the net adsorption remains negative. In ion-water clusters, even the smaller chloride anion prefers to lie closer to the surface.^{14,15} It has been hypothesized that a polarizable particle, like a large anion, prefers to be situated in a heterogeneous environment such as an interface in order to increase its polarization, but the question of whether polarization must be explicitly included in the force field in order to properly predict these results is still hotly debated.¹⁶⁻¹⁸ More careful parameterization of the ion size in particular has been shown to reproduce the interfacial adsorption of I^- without the need for explicit polarizability.¹⁹⁻²¹ Indeed, ion size has been shown to play a key role in driving ion accumulation at the interface. Generally, models with explicit polarizability included produce a stronger adsorption at the water liquid-vapour interface.²²

Alkali cations, too, have some variation in their affinity for the solution/air interface. Here, however, it is the small Li^+ ion which shows anomalous behaviour. Although it remains separated from the surface by at least one layer of water, recent computations using intrinsic density profiles have shown that Li^+ prefers to lie significantly closer to the interface than other alkali cations.²¹ This behavior might be connected with viewing Li^+ not as a single small cation, but as an extended ion including four tightly bound water molecules which effectively acts as a larger cation under some circumstances.^{21,23-25} However, questions about the relative stability of the water structure around the Li^+ ion²⁵⁻²⁷ and even whether the Li^+ -water coordination number is 4 or 6^{23,25,28-32} remain to be answered, before the more complicated issue of the ion at the air-water interface can be considered. As in the case of the anions, explicit polarizability may be important as well, but in this case it is the polarization of the solvent molecules at short separations from the small Li^+ ion that is crucial.^{32,33}

In this work, we pursue accurate density functional theory (DFT) and *ab initio* calculations of the equilibrium structures and energetics of Li^+ with either four or six associated water molecules. We carefully test a variety of calculation methods and basis sets, including the effects of basis set superposition error (BSSE) to ensure the accuracy of our results, and we compare these with the previous work on Li^+ -water clusters available in the litera-

ture.^{23,34-36} In addition, we apply an external electric field to the clusters. Understanding the effect of an electric field on small ion clusters is of great interest for elucidating at a molecular level the process of electrospray ionization (ESI), a topic that has been much studied *via* computer simulation in recent years,³⁷⁻³⁹ and more generally is also relevant to technological applications based on electrochemical cells.

It is also clear that an electric potential gradient exists across the water/air interface,^{21,40} highlighting the importance of electrostatic correlations in interfacial regions. Understanding the behaviour of the Li⁺-water clusters at equilibrium, and under electrostatic fields, should help to improve the description of the stability of the ion solvation shell in a low coordination environment such as the one found in liquid-vapour interfaces, as well as to provide insight into the behaviour of ions at interfaces under non-equilibrium conditions.⁴¹

The paper is structured as follows. We start by describing the computational details, including a discussion of the density functionals and basis sets employed here. A validation of the level of theory and basis sets follows. We then discuss our results for Li⁺-water clusters at equilibrium, both with and without applied electrostatic fields, and we perform a fitting of partial charges to the electrostatic potential surface (ESP) in order to gauge the ability of classical force fields to reproduce our DFT results. A final section with our conclusions and final remarks closes the paper.

2 Computational details

For basis sets we use the correlation consistent basis sets of Dunning *et al.*,⁴² cc-pVXZ and aug-cc-pVXZ. By systematically increasing the basis set as X=D, T, Q and 5 we can verify at what point we obtain converged energies with respect to the one-electron basis. To include electron correlation we compare the coupled-cluster with singles and doubles excitations (CCSD)^{43,44} *ab initio* methodology with two different density functional theory approaches, PBE⁴⁵ and SSB-D,^{46,47} the latter of which is an extension of PBE which incor-

porates Grimme’s dispersion correction in the functional.^{48,49} The SSB-D functional is thus included to investigate the contribution of dispersion interactions, which are expected to be unimportant for Li⁺-water interactions but may be significant for water-water interactions in the Li⁺-water clusters. In one of the geometries optimized by the CCSD method, we also carried out a calculation which includes triplet excitations perturbatively (CCSD(T)).⁵⁰

BSSE was corrected for using the counterpoise correction method,⁵¹ where energies of each component of the non-covalently bonded system are computed using the full set of basis functions of the whole system. BSSE has for a long time been recognized as a problematic issue in quantum chemical calculations of weak interactions, such as for example hydrogen bonding in the water dimer.⁵²⁻⁵⁵ In this work, the geometries are optimized without the BSSE correction, and the BSSE correction to the energy is included in subsequent single-point calculations.

An electric field can be applied to the systems in a simple manner by placing a positive and negative charge $\pm q$ equidistant from the Li⁺ ion and constraining the ion to be stationary in subsequent computations. The applied dipolar field strength E at the ion is then given by $E = 2kq/d^2$ with $k = 8.988 \times 10^9 \text{ Nm}^2/\text{C}^2$, and this is the quantity we will refer to as the field strength E in the remainder of the paper. Placing the charges at a distance $d = \pm 20 \text{ \AA}$ from the ion generates an electric field from the negative to the positive ion which varies less than 20% within 5 \AA of the ion. Charge magnitudes from $\pm 0.5e$ to $\pm 15e$ lead to field strengths in the 0.05 to 1.0 V/ range. All computations were done with the standard version of NWCHEM v6.3,⁵⁶ except for some molecular dynamics (MD) simulations and energy minimizations which were done with LAMMPS.⁵⁷ The geometry optimizations were done with the DRIVER algorithm in NWCHEM and “tight” convergence criteria.

3 Results

3.1 Validation of basis sets and level of theory

We validate our choice of basis set and level of theory for the subsequent calculations on larger clusters by systematically testing a series of basis sets, including the effects of BSSE, using both the PBE and SSB-D density functionals and also the CCSD method. Our test systems include monomers of both water and the Li^+ ion, water dimers,⁵⁵ and Li^+ bound to a single water molecule. Extension of the level of theory to the CCSD(T) level as well as extrapolation to the estimated basis set limit⁵⁸ led to changes of only ~ 1 kJ/mol in the $\text{Li}^+\cdot\text{H}_2\text{O}$ binding energy. All of these results are shown in Tables 1 and 2.

Our results show that the CCSD calculations are quite sensitive to BSSE, even with very large basis sets, whereas the PBE and SSB-D methods show negligible BSSE provided the basis sets are sufficiently large. We also note a surprisingly large effect of the basis set size on the lithium ion in particular, where using the cc-pV5Z basis set was necessary to obtain well converged results. This led us to consider mixed basis sets, where the O and H atoms are modelled with somewhat smaller basis sets. Our ultimate choices for methods and basis sets to use in the calculations on larger Li^+ -water clusters are therefore the PBE and SSB-D density functional methods, with the cc-pV5Z basis set on Li^+ and the aug-cc-pVTZ basis set on O and H atoms. The dispersion correction is around -0.6 kJ/mol for both $\text{Li}^+\cdot\text{H}_2\text{O}$ and the water dimer. Relative to the total interaction energy of the complexes, the dispersion correction is much more important for the water dimer than for the Li^+ -water complex, as expected.

We have also obtained the zero point vibrational energy (ZPVE) by computing the harmonic vibrational frequencies of the complexes and a single water molecule. The magnitude of the correction is significant in both complexes, being $\sim 28\%$ of the total interaction energy in the case of the water dimer and $\sim 5.5\%$ in the case of $\text{Li}^+\cdot\text{H}_2\text{O}$.

Table 1: Interaction potential energies U between H_2O molecules in the dimer and between Li^+ and one H_2O molecule in units of kJ/mol. “BSSE” designates computations where the basis set superposition error has been corrected for as described in the text. The “mixed” basis sets denote computations using the cc-pV5Z basis set for Li^+ and the aug-cc-pVXZ (X=D,T,Q) basis set for H_2O .

Theory	Basis set	$\Delta U(\text{Li}^+\cdot\text{H}_2\text{O})$	$\Delta U(\text{Li}^+\cdot\text{H}_2\text{O})$	$\Delta U(2\text{H}_2\text{O})$	$\Delta U(2\text{H}_2\text{O})$
			BSSE		BSSE
PBE	cc-pVDZ	-183.92	-158.47	-38.68	-19.30
	cc-pVTZ	-159.76	-146.95	-28.67	-20.78
	cc-pVQZ	-153.62	-146.82	-25.29	-21.08
	cc-pV5Z	-147.45	-145.97	-22.49	-21.38
	aug-cc-pVDZ	-140.17	-139.27	-22.07	-21.39
	aug-cc-pVTZ	-144.59	-143.93	-21.32	-21.38
	aug-cc-pVQZ	-146.49	-145.45	-21.38	-21.50
	mixed, X=D	-150.04	-144.92		
	mixed, X=T	-145.81	-145.58		
	mixed, X=Q	-145.57	-145.56		
SSB-D	cc-pVDZ	-180.17	-157.59	-38.76	-17.39
	cc-pVTZ	-161.30	-148.16	-30.15	-21.17
	cc-pVQZ	-154.68	-147.43	-26.02	-21.60
	cc-pV5Z	-147.57	-146.42	-22.94	-21.85
	aug-cc-pVDZ	-142.46	-139.86	-22.63	-21.67
	aug-cc-pVTZ	-145.97	-144.87	-21.82(-15.72 ^a)	-21.76
	aug-cc-pVQZ	-148.17	-146.04	-22.16	-22.13
	mixed, X=D	-150.78	-145.36		
	mixed, X=T	-146.29(-138.24 ^a)	-146.05		
	mixed, X=Q	-146.27	-146.13		
CCSD	cc-pVDZ	-172.91	-152.00	-29.03	-14.73
	cc-pVTZ	-156.66	-142.83	-24.30	-17.67
	cc-pVQZ	-154.04	-145.18	-21.64	-18.91
	cc-pV5Z	-153.19		-20.56	
	Q5 fit ^b	-154.33		-20.46	
	aug-cc-pVDZ	-150.03	-137.16	-21.27	-17.86
	aug-cc-pVTZ	-150.77	-141.68	-22.64	-19.18
	aug-cc-pVQZ	-155.59	-144.75	-20.70	-19.73
	mixed, X=D	-163.82	-142.71		
	mixed, X=T	-154.92 (-153.87 ^c)	-144.44		
mixed, X=Q	-154.08	-145.54			
Experiment			-142.3 ^d		-22.6 ^e

^a ZPVE subtracted.

^b Extrapolation to the basis set limit from results with cc-pVQZ and cc-pV5Z basis sets.⁵⁸

^c CCSD(T) result.

^d Ref. 59

^e Refs. 60,61

Table 2: Selected geometric quantities from test system calculations. All distances are in Ångstroms, all angles are in degrees. The “mixed” basis sets designate computations using the cc-pV5Z basis set for Li⁺ and the aug-cc-pVXZ (X=D,T,Q) basis set for H₂O.

Theory	Basis set	H ₂ O		Li ⁺ ·H ₂ O			2H ₂ O	
		d_{OH}	\angle_{HOH}	$d_{\text{Li-O}}$	d_{OH}	\angle_{HOH}	$d_{\text{O...O}}$	$\angle_{\text{O...HO}}$
PBE	cc-pVDZ	0.977	101.67	1.851	0.980	104.45	1.890	166.62
	cc-pVTZ	0.970	103.53	1.840	0.973	105.30	1.920	169.34
	cc-pVQZ	0.969	103.93	1.830	0.973	105.24	1.921	170.47
	cc-pV5Z	0.969	104.16	1.830	0.973	105.23	1.925	171.93
	aug-cc-pVDZ	0.973	103.80	1.856	0.976	104.80	1.915	170.89
	aug-cc-pVTZ	0.970	104.16	1.838	0.974	105.21	1.922	170.83
	aug-cc-pVQZ	0.969	104.18	1.832	0.973	105.23	1.925	170.97
	mixed, X=D			1.826	0.976	104.84		
	mixed, X=T			1.830	0.974	105.22		
	mixed, X=Q			1.833	0.973	105.29		
SSB-D	cc-pVDZ	0.962	101.15	1.845	0.964	104.15	2.079	125.89
	cc-pVTZ	0.956	102.76	1.829	0.958	104.95	1.957	162.87
	cc-pVQZ	0.955	103.22	1.829	0.957	104.94	1.958	167.63
	cc-pV5Z	0.955	103.43	1.829	0.958	104.93	1.961	172.77
	aug-cc-pVDZ	0.958	103.05	1.849	0.960	104.52	1.959	167.18
	aug-cc-pVTZ	0.956	103.41	1.829	0.959	104.91	1.961	168.38
	aug-cc-pVQZ	0.955	103.47	1.824	0.958	104.96	1.965	168.50
	mixed, X=D			1.816	0.960	104.58		
	mixed, X=T			1.824	0.959	104.93		
	mixed, X=Q			1.825	0.957	109.97		
CCSD	cc-pVDZ	0.964	102.21	1.867	0.969	104.28	1.969	173.97
	cc-pVTZ	0.956	104.04	1.833	0.960	105.39	1.965	175.71
	cc-pVQZ	0.955	104.40	1.821	0.958	105.42	1.968	173.59
	cc-pV5Z	0.954	104.80	1.820	0.958	105.47	1.971	172.45
	aug-cc-pVDZ	0.964	104.15	1.807	0.968	104.47	1.976	172.33
	aug-cc-pVTZ	0.956	104.59	1.815	0.960	105.19	1.956	173.46
	aug-cc-pVQZ	0.955	104.73	1.802	0.959	105.41	1.963	172.27
	mixed, X=D			1.793	0.968	105.18		
	mixed, X=T			1.804	0.961	105.42		
	mixed, X=Q			1.810	0.959	105.40		

3.2 $\text{Li}^+ \cdot 4\text{H}_2\text{O}$

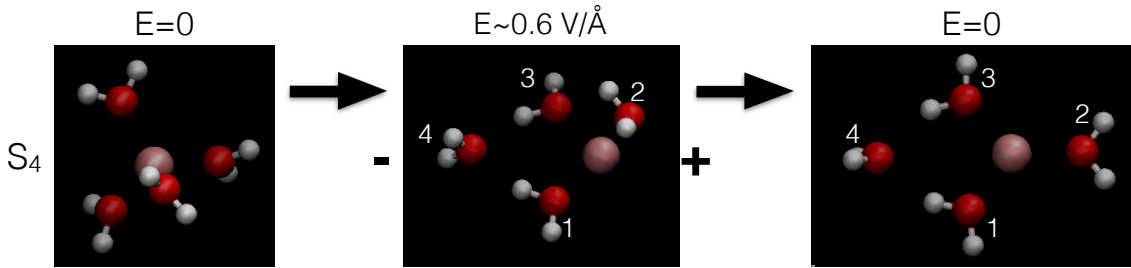


Figure 1: Snapshots of optimized geometries of the $\text{Li}^+ \cdot 4\text{H}_2\text{O}$ cluster with the SSB-D functional and the cc-pV5Z basis set for Li^+ and the aug-cc-pVTZ basis set for water. From L to R: 1) zero field, S_4 configuration. 2) field strength $E = 0.58 \text{ V/\AA}$. 3) reoptimization after removal of field. Labels match the molecule numbers in Table 4.

In agreement with previous results,^{23,34,35} we determine the global minimum for the cluster of four water molecules with Li^+ to have an S_4 symmetry. The water molecules arrange themselves in a configuration where the molecular dipoles point approximately along the Li^+ -O vectors. When an electric field is applied, however, this symmetry is no longer maintained and in Figure 1 we show snapshots of the optimized configurations of the $\text{Li}^+ \cdot 4\text{H}_2\text{O}$ cluster as the electric field is varied. At a critical field strength $\sim 0.5 \text{ V/\AA}$, the exact value of which depends somewhat on the field direction and initial symmetry, there is a breakdown in the coordination of water around the Li^+ ion and one of the waters becomes bound to one of the other water molecules instead in order to maximize its favourable orientation in alignment with the electric field. It is not surprising that this should occur at a high field strength, but what is more remarkable is that this asymmetric configuration with only three coordinated water molecules is actually the global minimum down to quite low field strengths. In Figure 2 we plot the minimum energy obtained after geometry optimization as a function of the electric field magnitude at the Li^+ ion. If the asymmetric configuration obtained at the high field strength is used as the starting point, and the optimization is then converged at lower field strengths, the asymmetric configuration has a lower minimum energy above $\sim 0.15 \text{ V/\AA}$ with the SSB-D functional. With the PBE functional, even in the absence of an applied field the asymmetric configuration is only 0.74 kJ/mol in energy

above the four-coordinated S_4 result, and a comparatively weak field of less than $0.1 \text{ V}/\text{\AA}$ is sufficient to make this state the global minimum. We note that others have also computed the energetics of these three-coordinated configurations^{23,36} in the absence of the applied field and have also noted the closeness of the energy levels. The binding energy per water molecule is tabulated in Table 3. We note that some of the electrostatic fields we employ here are stronger than the field $\sim 0.35 \text{ V}/\text{\AA}$ that caused protons to dissociate from water molecules in previous DFT based *ab initio* MD simulations.⁶² We did not observe any dissociation events in any of our calculations, likely due to a comparatively high energy barrier which must be overcome for such an event to be observed.

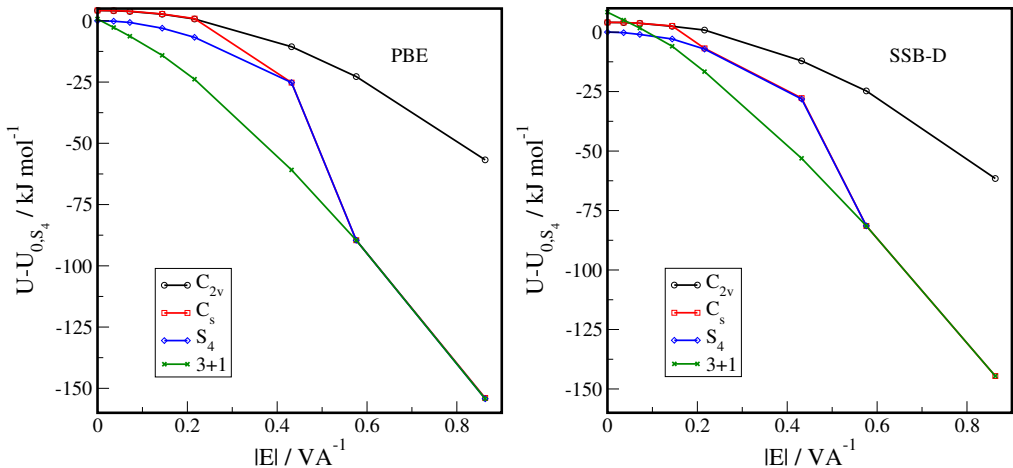


Figure 2: Plots of $U - U_{S_4}$, the difference in binding potential energy between the optimized geometry at the indicated field strength and the global minimum geometry in zero field in the S_4 symmetry ($-312.94236 E_h$ in the PBE calculations with the mixed basis set described in the text, and $-315.52698 E_h$ in the SSB-D case). The legend indicates the symmetry of the initial configuration before geometry optimization. The C_{2v} and C_s configurations are distinguished by the direction of the applied electrostatic field.

A field strength of $0.15 \text{ V}/\text{\AA}$ remains quite high, however field strengths of this size are relatively common in some contexts, *e.g.* in ion channels in cell membranes⁶⁵ or at the tip of an atomic force microscope.⁶⁶ In fact, the electric field at an ordinary air-water interface has been calculated using the SPC/E water model and an intrinsic surface analysis to be on the order of $0.1 \text{ V}/\text{\AA}$.²¹ Since this field only exists in a very narrow region of the interface and has a high gradient, one should be cautious when making comparisons with the extended

Table 3: Binding energy $\Delta U_{\text{bind}} = U_{\text{clust}} - nU_{\text{H}_2\text{O}} - U_{\text{Li}^+}$ (in kJ/mol) per water molecule in $\text{Li}^+ \cdot n\text{H}_2\text{O}$ clusters. N_c refers to the water coordination number of Li^+ . All results are in zero applied electric field. Results in parentheses have subtracted the zero point vibrational energy (ZPVE) computed with the cc-pVQZ basis set on Li^+ and the aug-cc-pVTZ basis set on O and H. The MD result is from energy minimization with classical force fields (SPC/E⁶³ for water, Dang’s model⁶⁴ for Li^+).

Cluster	PBE	SSB-D	MD	Ref. 35	Ref. 36	Ref. 23	Experiment ⁵⁹
$\text{Li}^+ \cdot 3\text{H}_2\text{O}$, D_3	-121.5	-124.6		-130.6	-118.3	-117.2	-112.3
$\text{Li}^+ \cdot 3\text{H}_2\text{O}$, $N_c = 2$	-112.4	-114.5			-111.7	-107.1	
$\text{Li}^+ \cdot 4\text{H}_2\text{O}$, S_4	-107.8	-112.5(-104.4)	-117.2	-116.4	-105.2	-105.0	-101.4
$\text{Li}^+ \cdot 4\text{H}_2\text{O}$, $N_c = 3$	-107.6	-110.4(-101.1)	-110.9		-104.0	-102.3	
$\text{Li}^+ \cdot 6\text{H}_2\text{O}$, C_1	-83.5	-91.8			-79.6		-85.7
$\text{Li}^+ \cdot 6\text{H}_2\text{O}$, T_h	-82.3	-90.4					
$\text{Li}^+ \cdot 6\text{H}_2\text{O}$, $N_c = 5$	-85.9	-92.1					
$\text{Li}^+ \cdot 6\text{H}_2\text{O}$, $N_c = 4$	-90.1	-94.5			-90.2	-84.2	
$\text{Li}^+ \cdot 6\text{H}_2\text{O}$, $N_c = 2$	-84.6						

electrostatic field we study in this work. Nevertheless, these surprising results should be considered in the picture of a stable $\text{Li}^+ \cdot 4\text{H}_2\text{O}$ structure which acts as a single unit near the water-air interface, particularly under the influence of strong external fields.

We have computed the zero-point vibrational energy (ZPVE) of the S_4 symmetric configuration and the 3-coordinated configuration by computing the harmonic vibrational frequencies of the complexes and of a single water molecule. The ZPVE from a SSB-D calculation using the cc-pVQZ basis set on Li^+ and the aug-cc-pVTZ basis set on hydrogen and oxygen atoms is 257.4 kJ/mol, and the ZPVE of one H_2O molecule with the aug-cc-pVTZ basis set is 56.3 kJ/mol. Therefore, we obtain the total ZPVE contribution to the binding energy of the S_4 symmetric $\text{Li}^+ \cdot 4\text{H}_2\text{O}$ cluster to be 32.4 kJ/mol or 8.1 kJ/mol per water molecule, or 7.2% of the binding energy -112.5 kJ/mol at the same level of theory and basis set. For comparison, the ZPVE arising from the intramolecular vibrations in the water dimer (see Table 1) is around 6.1 kJ/mol or 28% of the total interaction energy. If the ZPVE is not considered when describing the energetics and dynamics of *e.g.* water exchange in and out of the solvation shell, then we might expect slower residence times and stronger binding in classical MD simulations based on force fields parameterized based on DFT or *ab initio* re-

sults. This could be one possible explanation for the larger coordination numbers predicted by some of the classical MD simulations of aqueous Li^+ .³⁰ One route forward to explicitly including ZPVE corrections in MD simulations is by methods like path-integral MD⁶⁷ or centroid MD.⁶⁸ ZPVE corrections may also be implicitly included in empirical force fields parameterized against experimental data, *e.g.* binding energies, however many experimental determinations of binding energies also implicitly include the ZPVE, including those cited in the present work.⁵⁹⁻⁶¹

Energy minimization of $\text{Li}^+ \cdot 4\text{H}_2\text{O}$ with empirical models (SPC/E model⁶³ for water, and Dang’s model⁶⁴ for Li^+) led to a much larger difference in binding energies between the S_4 symmetry and the $3 + 1$ configuration with one detached water than we and others observe in the DFT calculations. We completed additional classical MD simulations of the $\text{Li}^+ \cdot 4\text{H}_2\text{O}$ clusters with one detached water in the NVT ensemble at $T = 300$ K to estimate the relative stability of this configuration. We note that the concept of a constant temperature is inherently problematic with such a small number of particles; in practice the temperature varied by ± 100 K over the course of the simulations. The time at which the configuration transitioned to the S_4 symmetry varied greatly, being as low as 3 ps and as high as 92 ps over the course of ten trial runs. Overall, the average transition time was 47 ± 34 ps, demonstrating that these configurations with reduced symmetry can remain stable for significant time periods, and that the transformation from one structure to the other is an activated process. We note that the MD simulations were performed with a non-polarizable forcefield. The similar behavior observed in our classical MD simulations indicates that polarization effects do not influence the relative stability of the cluster. Hence this offers the prospect of investigating the energetics and structure of these small clusters with widely accepted non-polarizable forcefields, which do not incorporate explicitly electronic degrees of freedom. This question, particularly the charge distribution in the Li^+ cluster is discussed in more detail in the following section.

3.3 ESP fitting of partial charges

In order to assess the ability of classical models to reproduce our DFT results, we have computed the electrostatic potential (ESP) surface and found the set of partial charges on the atomic sites that can best fit the electrostatic potential in the cluster. All of these fits were done on the $\text{Li}^+ \cdot 4\text{H}_2\text{O}$ clusters using the default parameters in the NWCHEM ESP routine.⁶⁹ We did these fits using two different sets of constraints, one where only the Li^+ charge was set to be 1.0, and another where in addition all O and all H charges were each constrained to be equal, as they would be in a typical classical force field. All of these results are shown in Table 4.

The largest deviations between the ESP resulting from the partial charge fittings and the DFT results are for the $3 + 1$ configuration in the absence of external field. It is remarkable that the constrained fits (see set of data 2 in Table 4), which do not allow differing partial charges on atoms of the same type, do not result in a significantly worse fitting. This would suggest that fluctuating charge models⁷⁰ might not be required to describe the energetics of the asymmetric configuration, and instead improvements should be sought from semiclassical models which include atomic polarizability in an approximate way.⁷¹

Deviations in the asymmetric case notwithstanding, the partial charge models provide a very good description of the ESP, with mean-square deviations at each grid point ~ 0.2 to 0.3 kJ/mol from the DFT results. The water molecules in the Li^+ clusters are found to have effective partial charges, and hence dipole moments, much greater than would be seen in an isolated water molecule, owing to the polarizing influence of the lithium ion. For comparison, we obtained results of $q_O = -0.644e$ and $q_H = 0.322e$ for the isolated water molecule with the SSB-D functional and the aug-cc-pVTZ basis set.

3.4 $\text{Li}^+ \cdot 6\text{H}_2\text{O}$

We find a stable local minimum for the cluster with six water molecules in a C_1 symmetry with a Li^+ -water coordination number of 6, however this is not the global minimum geometry. As

Table 4: Results of fitting partial charges to the electrostatic potential (ESP) at geometries optimized starting from either the S_4 or the asymmetric $3 + 1$ configurations in the absence of field, followed by the application of the external electric field (*cf.* Figure 1). Molecules are labelled as shown in Figure 1. The fourth water molecule is the detached water in the $3 + 1$ configurations. ‘‘RMSD’’ denotes the root mean squared deviation between the fitted ESP and the DFT results across all grid points in kJ/mol. All data were obtained using SSB-D functionals and the mixed basis set described in the text. All charges are given in terms of the fundamental charge $e = 1.602 \times 10^{-19}$ C. The partial charges for molecules 2 through 4 in the S_4 zero field case are the same as those of the 1st molecule.

initial state:	S_4	S_4	S_4	$3 + 1$	$3 + 1$	$3 + 1$	$3 + 1$
$E/\text{V}\text{\AA}^{-1}$:	zero	0.14	0.22	zero	0.14	0.22	0.43
1) Constrain $\text{Li}^+ q = 1.0e$							
O_1	-0.863	-0.877	-0.840	-0.948	-0.962	-0.978	-0.977
H_{11}	0.428	0.427	0.411	0.447	0.474	0.475	0.473
H_{12}	0.435	0.444	0.432	0.437	0.443	0.450	0.459
O_2	"	-0.816	-0.814	-0.917	-0.905	-0.855	-0.841
H_{21}		0.406	0.405	0.452	0.449	0.430	0.430
H_{22}		0.432	0.430	0.439	0.451	0.430	0.424
O_3		-0.867	-0.845	-0.933	-0.961	-0.996	-1.058
H_{31}		0.441	0.432	0.421	0.446	0.461	0.500
H_{32}		0.423	0.412	0.455	0.473	0.481	0.491
O_4		-0.898	-0.934	-0.443	-0.685	-0.650	-0.721
H_{41}		0.444	0.458	0.300	0.384	0.371	0.410
H_{42}		0.442	0.452	0.290	0.394	0.382	0.412
RMSD	0.174	0.171	0.176	0.549	0.231	0.237	0.222
% dev.	1.42	1.39	1.42	7.06	2.08	2.10	1.89
2) Constrain $\text{Li}^+ q = 1.0e$, all O and H charges equal							
O	-0.864	-0.863	-0.850	-0.931	-0.960	-0.958	-0.996
H	0.432	0.432	0.425	0.466	0.480	0.479	0.498
RMSD	0.175	0.179	0.188	0.642	0.280	0.308	0.310
% dev.	1.43	1.53	1.65	7.63	2.31	2.47	2.67

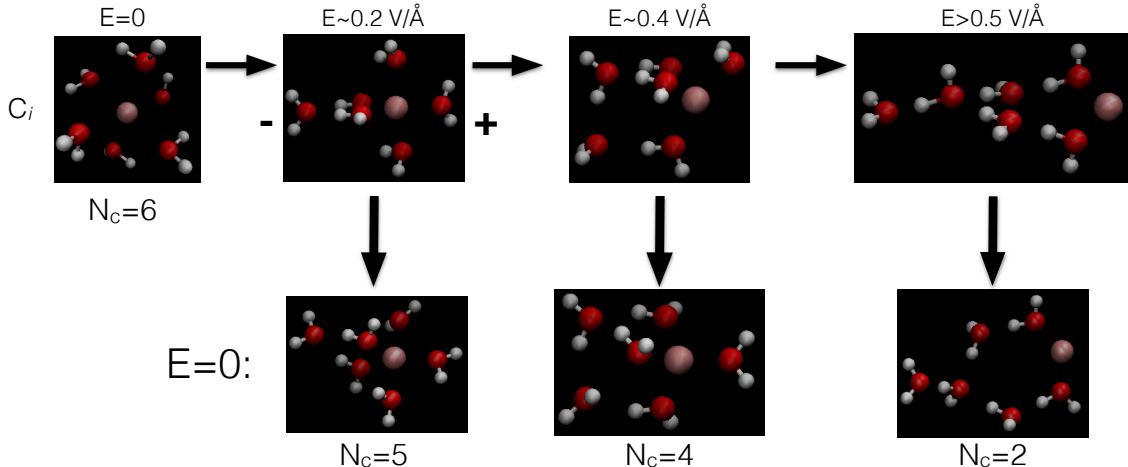


Figure 3: Snapshots of optimized geometries of the $\text{Li}^+ \cdot 6\text{H}_2\text{O}$ cluster. The top row shows configurations obtained starting from the C_i configuration as electric field strength is increased. The bottom row shows configurations obtained after removing the applied field, starting from the respective configurations with reduced ion coordination numbers N_c . The functional and basis sets are identical to those used for the $\text{Li}^+ \cdot 4\text{H}_2\text{O}$ configurations shown in Figure 1.

in the smaller four water cluster, we can alter the 6-coordinated configuration by application of an electric field. Due to the greater number of configurations available to the larger cluster, there is more variability in the final geometries obtained, dependent on factors such as the symmetry of the initial configuration and the direction of the applied field. Snapshots of a set of optimized configurations obtained in one series of calculations are displayed in Figure 3. Configurations with 1 or 2 detached water molecules are produced for fields in the 0.1 to 0.2 V/\AA range, and in the case of the PBE functional, with four detached water molecules at somewhat higher fields ($\sim 0.5 \text{ V/\AA}$). The elongated configurations of water molecules in the high fields with ordered dipoles are similar to those seen in simulations of small water clusters in applied fields of similar size (0.15 V/\AA).⁷² When these configurations are reoptimized in the absence of applied field, we find that the configuration with $N_c = 4$ is the global minimum. The arrangement of the water molecules around the ion is nonetheless different from the one found above for the $\text{Li}^+ \cdot 4\text{H}_2\text{O}$ cluster. The formation of hydrogen bonds with the two molecules not directly coordinated to Li^+ induces a reorientation of the dipoles of the water molecules taking part in the tetrahedral cluster. These dipoles do not orient along the $\text{Li}^+\text{-O}$

vectors. This structure may be representative of an asymmetric coordination environment, such as that present at liquid-vapor interfaces. It has been recently found in classical MD simulations that lithium-water clusters adsorb at the water surface in a configuration where the clusters are oriented with one of the water molecules facing the vapor phase at the edge of the outermost interfacial layer of water.²¹

The minimum configurational energies as a function of the applied field and for different initial configurations are plotted in Figure 4 and binding energies per water molecule are reported in Table 3. As in the cluster with four water molecules, the SSB-D functional slightly reduces the preference for less symmetric or less coordinated structures versus the PBE results. However, the qualitative trends are the same. Again, as noted above, we do not find evidence for dissociation of water molecules induced by the application of the electrostatic field.

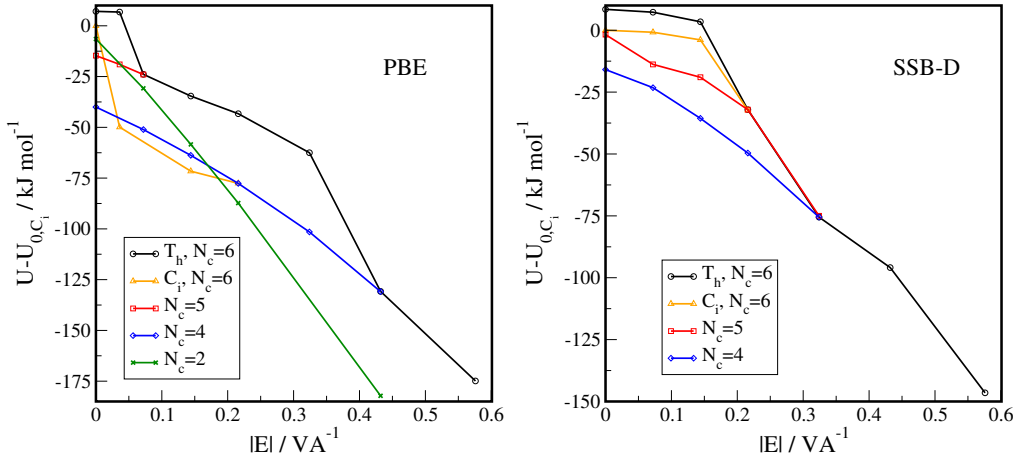


Figure 4: Plots of $U - U_{C_i}$, the difference in potential energy between the optimized geometry at the indicated field strength and the global minimum geometry in zero field in the $N_c = 6$, C_i symmetry ($-465.72962 E_h$ in the PBE calculations with the mixed basis set described in the text, and $-469.55557 E_h$ in the SSB-D case). The legend indicates the symmetry of the initial configuration before geometry optimization.

4 Conclusions

We have undertaken extensive computations of small clusters of lithium ions and water ($\text{Li}^+ \cdot n\text{H}_2\text{O}$, $n = 4, 6$). We have carefully tested for basis set superposition error (BSSE) and considered extrapolation to the basis set limit. We find that *ab initio* CCSD calculations are quite sensitive to BSSE, even with very large basis sets, whereas the PBE and SSB-D methods show negligible BSSE provided sufficiently large basis sets are used. Our DFT results for $\text{Li}^+ \cdot \text{H}_2\text{O}$ as well as the water dimer show that the combination of mixed basis sets (aug-cc-pVTZ on water atoms, cc-pV5Z on Li^+) with the SSB-D functionals can compute the interaction energies with an error of less than 2 kJ/mol with respect to the energies obtained from high level *ab initio* methods.

Our results on larger clusters with 4 or 6 water molecules agree well with previous work in the literature. We confirm that a cluster of four water molecules bound to the Li^+ ion is far more stable (-113 kJ/mol per water molecule) than a cluster with 6 water molecules directly bound to the ion (-92 kJ/mol per water molecule). Our results provide more support for a coordination number of 4 rather than 6, which is consistent with recent molecular dynamics simulations of aqueous solutions using empirical force-fields. We find that the contribution of the zero point vibrational energy (ZPVE) to the binding energy of Li^+ -water clusters is significant (8.1 kJ/mol per , or $\sim 7\%$ of the total) but not as great a proportion as has been found for the water dimer (6.1 kJ/mol per water molecule, or $\sim 28\%$ of the total).

We have further estimated the atomic partial charges on the water molecules by fitting these to the electrostatic potential surface using different charge constraint schemes, whereby the charges in the water molecules are left as free parameters or fixed to adopt the same value in atoms of the same element. Interestingly, we found that the constraining scheme does not have a major impact on the quality of the fit to the electrostatic potential surface, which would indicate that fluctuating charge models are not essential to describe the electrostatic environment generated by these clusters. On the other hand we found that the fitting of the ESP of $\text{Li}^+ \cdot 4\text{H}_2\text{O}$ clusters using atomic charges is worse for asymmetric configurations, *e.g.*

what we have termed the 3 + 1 configuration, where the coordination shell is disrupted with respect to a symmetric tetrahedral arrangement. This result shows a limitation of the charge fitting approach employed here, where the charges are located at the atomic sites. We note that state of the art water models, *e.g.* TIP4P, have highlighted the need to shift the position of the oxygen charge along the water HOH bisector. This strategy may result in a better fit of the electrostatic surface potential with point charges.

Additionally, we considered the impact of an electric field on the structure of Li⁺-water clusters. In general, application of an electric field biases the molecular configurations around the ion towards lower coordination numbers. Of particular interest is the fact that an asymmetric configuration of three water molecules bound to the ion with the additional water molecule in a second solvation shell is actually the minimum energy configuration in a field magnitude $|E| \gtrsim 0.15 \text{ V/\AA}$. This is a large field strength but such fields are relevant in some systems, *e.g.* at a water-air interface or in electrospray ionization. In the ESP fits the application of the electrostatic field slightly shifts the values of oxygen and hydrogen atomic charges with respect to those obtained in the absence of field. Although the shift is small, our results indicate that accurate computations might benefit from the consideration of polarizable forcefields. Further work should serve to elucidate the relevance of our results to better explanations of the behaviour of lithium ions in aqueous solution and aqueous solution interfaces.

Acknowledgement

We thank The Research Council of Norway (Project 221675) and the EPSRC (EP/J003859/1) for financial support, and NOTUR (account nn2920k) for computational resources. F.B. acknowledges the award of an EPSRC Leadership Fellowship.

References

- (1) Heydweiller, A. *Ann. Phys.* **1910**, *33*, 145–185.

- (2) Jones, G.; Ray, W. A. *J. Am. Chem. Soc.* **1937**, *59*, 187.
- (3) Onsager, L.; Samaras, N. N. T. *J. Phys. Chem.* **1934**, *2*, 528.
- (4) Jungwirth, P.; Tobias, D. J. *J. Phys. Chem. B* **2001**, *105*, 10468–10472.
- (5) Dang, L. X.; Chang, T. M. *J. Phys. Chem. B* **2002**, *106*, 235–238.
- (6) Jungwirth, P. *Faraday Discuss.* **2009**, *141*, 9–30.
- (7) Caleman, C.; Hub, J. S.; van Maaren, P. J.; van der Spoel, D. *Proc. Nat. Acad. Sci.* **2011**, *108*, 6838–6842.
- (8) Bauer, B. A.; Ou, S.; Patel, S. *Chem. Phys. Lett.* **2012**, *527*, 22–26.
- (9) Tobias, D. J.; Stern, A. C.; Baer, M. D.; Levin, Y.; Mundy, C. J. *Ann. Rev. Phys. Chem.* **2013**, *64*, 339–359.
- (10) Liu, D.; Ma, G.; Levering, L. M.; Allen, H. C. *J. Phys. Chem. B* **2004**, *108*, 2252–2260.
- (11) Otten, D. E.; Shaffer, P. R.; Geissler, P. L.; Saykally, R. J. *Proc. Nat. Acad. Sci.* **2012**, *109*, 701–705.
- (12) Petersen, P. B.; Saykally, R. J. *Ann. Rev. Phys. Chem.* **2006**, *57*, 333–364.
- (13) Knipping, E. M.; Lakin, M. J.; Foster, K. L.; Jungwirth, P.; Tobias, D. J.; Gerber, R. B.; Dabdub, D.; Finlayson-Pitts, B. J. *Science* **2000**, *288*, 301.
- (14) Perera, L.; Berkowitz, M. L. *J. Chem. Phys.* **1991**, *95*, 1954–1963.
- (15) Koch, D. M.; Peslherbe, G. H. *Chem. Phys. Lett.* **2002**, *359*, 381–389.
- (16) Carignano, M. A.; Karlström, G.; Linse, P. *J. Phys. Chem. B* **1997**, *101*, 1142–1147.
- (17) Hagberg, D.; Brdarski, S.; Karlström, G. *J. Phys. Chem. B* **2005**, *109*, 4111–4117.

- (18) Horinek, D.; Herz, A.; Vrbka, L.; Sedlmeier, F.; Mamatkulov, S. I.; Netz, R. R. *Chem. Phys. Lett* **2009**, *479*, 173–183.
- (19) Eggimann, B.; Siepmann, J. I. *J. Phys. Chem. C* **2008**, *112*, 210–218.
- (20) Levin, Y.; dos Santos, A. P.; Diehl, A. *Phys. Rev. Lett.* **2009**, *103*, 257802.
- (21) Bresme, F.; Chacón, E.; Tarazona, P.; Wynveen, A. *J. Chem. Phys.* **2012**, *137*, 114706.
- (22) Jungwirth, P.; Tobias, D. J. *Chem. Rev.* **2006**, *106*, 1259–1281.
- (23) San-Román, M. L.; Carrillo-Tripp, M.; Saint-Martin, H.; Hernández-Cobos, J.; Ortega-Blake, I. *Theor. Chem. Acc.* **2006**, *115*, 117–189.
- (24) Wynveen, A.; Bresme, F. *J. Chem. Phys.* **2010**, *133*, 144706.
- (25) Zeng, Y.; Wang, C.; Zhang, X.; Ju, S. *Chem. Phys.* **2014**, *433*, 89–97.
- (26) Spångberg, D.; Rey, R.; Hynes, J. T.; Hermansson, K. *J. Phys. Chem. B* **2003**, *107*, 4470–4477.
- (27) Møller, K. B.; Rey, R.; Masia, M.; Hynes, J. T. *J. Chem. Phys.* **2005**, *122*, 114508.
- (28) Chandrasekhar, J.; Spellmeyer, D. C.; Jorgensen, W. L. *J. Am. Chem. Soc.* **1984**, *106*, 903–910.
- (29) Howell, I.; Nielson, G. W. *J. Phys. Condens. Matter* **1996**, *8*, 4455–4463.
- (30) Egorov, A. V.; Komolkin, A. V.; Chizhik, V. I.; Yushmanov, P. V.; Lyubartsev, A. P.; Laaksonen, A. *J. Phys. Chem. B* **2003**, *107*, 3234–3242.
- (31) Öhrn, A.; Karlström, G. *J. Phys. Chem. B* **2004**, *108*, 8452–8459.
- (32) Pejov, L.; Spångberg, D.; Hermansson, K. *J. Phys. Chem. A* **2005**, *109*, 5144–5152.
- (33) Masia, M.; Probst, M.; Rey, R. *J. Chem. Phys.* **2005**, *123*, 164505.

- (34) Feller, D.; Glendening, E. D.; Woon, D. E.; Feyerisen, M. W. *J. Chem. Phys.* **1995**, *103*, 3526.
- (35) Pye, C. C.; Rudolph, W.; Poirier, R. A. *J. Phys. Chem.* **1996**, *100*, 601–605.
- (36) Li, J.; Liu, T.; Li, X.; Ye, L.; Chen, H.; Fang, H.; Wu, Z.; Zhou, R. *J. Phys. Chem. B* **2005**, *109*, 13639.
- (37) Daub, C. D.; Cann, N. M. *Anal. Chem.* **2011**, *83*, 22393–22399.
- (38) Konermann, L.; McAllister, R. G.; Metwally, H. *J. Phys. Chem. B* **2014**, *118*, 12025–12033.
- (39) Consta, S.; Oh, M. I.; Soltani, S. *Int. J. Mass Spectrom.*, <http://dx.doi.org/10.1016/j.ijms.2014.09.004>.
- (40) Saykally, R. J. *Nature Chemistry* **2013**, *5*, 82–84.
- (41) Römer, F.; Wang, Z.; Wiegand, S.; Bresme, F. *J. Phys. Chem. B* **2013**, *117*, 8209–8222.
- (42) Woon, D. E.; Dunning, T. H. *Theor. Chem. Acc.* **1997**, *97*, 150–157.
- (43) Rendell, A. P.; Lee, T. J.; Komornicki, A.; Wilson, S. *Theor. Chem. Acc.* **1992**, *84*, 271–287.
- (44) Kobayashi, R.; Rendell, A. P. *Chem. Phys. Lett.* **1997**, *265*, 1–11.
- (45) Perdew, J. P.; Burke, K.; Ernzerhof, M. *Phys. Rev. Lett.* **1996**, *77*, 3865–3868.
- (46) Swart, M.; Solà, M.; Bickelhaupt, F. M. *J. Comput. Methods Sci. Eng.* **2009**, *9*, 69–77.
- (47) Swart, M.; Solà, M.; Bickelhaupt, F. M. *J. Chem. Phys.* **2009**, *131*, 094103.
- (48) Grimme, S. *J. Comput. Chem.* **2004**, *25*, 1463–1473.
- (49) Grimme, S. *J. Comput. Chem.* **2006**, *27*, 1787.

- (50) Raghavachari, K.; Trucks, G. W.; Pople, J. A.; Head-Gordon, M. *Chem. Phys. Lett.* **1989**, *157*, 479.
- (51) Boys, S. F.; Bernardi, F. *Mol. Phys.* **1970**, *19*, 553–566.
- (52) Newton, M. D.; Kestner, N. R. *Chem. Phys. Lett.* **1983**, *94*, 198–201.
- (53) Szalewicz, K.; Cole, S. J.; Kołos, W.; Bartlett, R. J. *J. Chem. Phys.* **1988**, *89*, 3662–3673.
- (54) Åstrand, P.-O.; Wallqvist, A.; Karlström, G. *J. Phys. Chem.* **1991**, *95*, 6395–6396.
- (55) Halkier, A.; Koch, H.; Jørgensen, P.; Christiansen, O.; Nielsen, I. M. B.; Helgaker, T. *Theor. Chem. Acc.* **1997**, *97*, 150–157.
- (56) Valiev, M.; Bylaska, E. J.; Govind, N.; Kowalski, K.; Straatsma, T. P.; van Dam, H. J. J.; Wang, D.; Nieplocha, J.; Apra, E.; Windus, T. L.; de Jong, W. A. *Comput. Phys. Commun.* **2010**, *181*, 1477.
- (57) Plimpton, S. J. *J. Comp. Phys.* **1995**, *117*, 1.
- (58) Halkier, A.; Helgaker, T.; Jørgensen, P.; Klopper, W.; Koch, H.; Olsen, J.; Wilson, A. K. *Chem. Phys. Lett.* **1998**, *286*, 243–252.
- (59) Džidić, I.; Kebarle, P. *J. Phys. Chem.* **1970**, *74*, 1466–1474.
- (60) Curtiss, L. A.; Frurip, D. J.; Blander, M. *J. Chem. Phys.* **1979**, *71*, 2703.
- (61) Reimers, J.; Watts, R.; Klein, M. *Chem. Phys.* **1982**, *64*, 95.
- (62) Saitta, A. M.; Saija, F.; Gianquinta, P. V. *Phys. Rev. Lett.* **2012**, *108*, 207801.
- (63) Berendsen, H. J. C.; Grigera, J. R.; Straatsma, T. P. *J. Phys. Chem.* **1987**, *91*, 6269.
- (64) Dang, L. X. *J. Chem. Phys.* **1992**, *96*, 6970.

- (65) Philippsen, A.; Im, W.; Engel, A.; Schimer, T.; Roux, B.; Müller, D. *J. Biophys. J.* **2002**, *82*, 1667–1676.
- (66) Guan, L.; Qi, G.; Liu, S.; Zhang, H.; Zhang, Z.; Yang, Y.; Wang, C. *J. Phys. Chem. C* **2009**, *113*, 661–665.
- (67) Berne, B. J.; Thirumalai, D. *Ann. Rev. Phys. Chem.* **1986**, *37*, 401.
- (68) Pavese, M.; Berard, D. R.; Voth, G. A. *Chem. Phys. Lett.* **1999**, *300*, 93–98.
- (69) Chipot, C.; Maignet, B.; Rivail, J.-L.; Scheraga, H. A. *J. Phys. Chem.* **1992**, *96*, 10276–10284.
- (70) Rick, S. W.; Stuart, S. J.; Berne, B. J. *J. Chem. Phys.* **1994**, *101*, 6141–6156.
- (71) Åstrand, P.-O.; Linse, P.; Karlström, G. *Chem. Phys.* **1995**, *191*, 195–202.
- (72) Vegiri, A. *J. Mol. Liq.* **2004**, *110*, 155–168.